Robotica (2007) volume 25, pp. 691–701. © 2007 Cambridge University Press
doi:10.1017/S0263574707003669 Printed in the United Kingdom

Geometry for robot path planning

Lyle Noakes* and Tomasz Popiel

School of Mathematics and Statistics, University of Western Australia, Nedlands, WA 6009 Perth, Australia.

(Received in Final Form: June 8, 2007. First published online: August 1, 2007)

SUMMARY

There have been many interesting recent results in the area of geometrical methods for path planning in robotics. So it seems very timely to attempt a description of mathematical developments surrounding very elementary engineering tasks. Even with such limited scope, there is too much to cover in detail. Inevitably, our knowledge and personal preferences have a lot to do with what is emphasised, included, or left out.

Part I is introductory, elementary in tone, and important for understanding the need for geometrical methods in path planning. Part II describes the results on geometrical constructions that imitate well-known constructions from classical approximation theory. Part III reviews a class of methods where classical *criteria* are extended to curves in Riemannian manifolds, including several recent mathematical results that have not yet found their way into the literature.

KEYWORDS: Path planning; Interpolation; Lie group; Lie quadratic; Asymptotic estimate; Rigid body.

1. Part I: Some Elementary Tasks

1.1. Introduction

Imagine a camera K free to rotate about a fixed point 0 in Euclidean 3-space E^3. Configurations and possibly angular velocities of K are specified at various times t_i. Our task is to move K while satisfying these constraints. To see the need for geometrical methods, we first try to adapt familiar methods from the approximation theory.

Let (x_1, x_2, x_3) be a positively oriented orthonormal frame of column vectors fixed relative to K at 0. At any time t, the configuration of K is given by the 3×3 orthogonal matrix

$$x(t) := [x_1 x_2 x_2]$$

where $\det(x(t))$ is identically 1. The path followed by K corresponds precisely to a curve x in the *rotation group* $SO(3)$ (the Lie group of 3×3 real orthogonal matrices of determinant 1). Angular velocities correspond precisely to vectors $\dot{x}(t)$ in the *tangent space* $TSO(3)_{x(t)}$ to $SO(3)$ at $x(t)$. Path planning for K amounts to selecting a curve x that satisfies the given constraints. This can be regarded as a kind of interpolation problem in $SO(3)$. We consider a very simple test problem in the following

Problem 1. $x(0)$ and $x(T)$ are given as $x_0, x_T \in SO(3)$ for some $T > 0$, with no other constraints. How should we choose our interpolant $x : [0, T] \to SO(3)$? □

If we were working in Euclidean space E^3 instead of $SO(3)$, we would almost surely choose the affine line from x_0 to x_T

$$x(t) = (1 - t/T)x_0 + (t/T)x_T.$$

However affine lines are unavailable in $SO(3)$. Indeed, although a 3×3 real matrix corresponds to a point in Euclidean 9-space E^9, an affine line in E^9 intersects the three-dimensional curved space $SO(3)$ in at the most two points. In effect, an affine line in E^9 is a curve of nonorthogonal matrices, which would have to be Gramm–Schmidt orthogonalised at every parameter value to yield a curve in $SO(3)$. Although conceptually simple, this would be computationally demanding and of doubtful practical value. The standard fix is

Method 1. *Noting that* $SO(3)$ *is* locally *equivalent to* E^3*, namely that* $SO(3)$ *is a* smooth three-manifold*, we can find an open cover of* $SO(3)$ *by* coordinate charts *diffeomorphic (smoothly equivalent) to open subsets of* E^3*. With luck,* x_0 *and* x_T *lie in a common chart, and the affine line in* E^3 *joining the images of* x_0 *and* x_T *is also contained in the image of the chart diffeomorphism. Then the inverse of the chart diffeomorphism maps the affine line to a* chart-based affine interpolant *in* $SO(3)$. □

Chart-based interpolants work reasonably well when coordinate charts are small and x_0, x_T are close, but their performance in general is poor:

* Corresponding author. E-mail: lyle@maths.uwa.edu.au

https://doi.org/10.1017/S0263574707003669 Published online by Cambridge University Press

Example 1. *The orthogonal matrix with* Euler angles $(\phi, \psi, \theta) \in (0, 2\pi) \times (0, 2\pi) \times (0, \pi)$ *is defined in section 15.6.4 of ref. [39] as:*

$$R(\phi, \psi, \theta) := \begin{bmatrix} \cos\psi\cos\phi - \cos\theta\sin\phi\sin\phi & \cos\psi\sin\phi + \cos\theta\cos\phi\sin\psi & \sin\theta\sin\phi \\ -\sin\psi\cos\phi - \cos\theta\sin\phi\cos\psi & -\sin\psi\sin\phi + \cos\theta\cos\phi\cos\psi & \sin\theta\cos\psi \\ \sin\theta\sin\phi & -\sin\theta\cos\phi & \cos\theta \end{bmatrix}.$$

Then R is a diffeomorphism onto the open dense subset U of SO(3) *comprising rotations whose last row is not* $\pm[0\ 0\ 1]$*, enabling U to be incorporated into a system of coordinate charts.*

For $j = 0, 1$ *let* x_{jT} *be the* 3×3 *orthogonal matrices:*

$$\frac{1}{4}\begin{bmatrix} (-1)^j 2\sqrt{3} & \sqrt{3} & 1 \\ -2 & (-1)^j 3 & (-1)^j\sqrt{3} \\ 0 & -2 & 2\sqrt{3} \end{bmatrix} \in U.$$

The chart diffeomorphism R^{-1} *maps* x_0 *and* x_T *to* $(0, \pi/6, \pi/6)$ *and* $(0, 5\pi/6, \pi/6)$*, respectively. The chart-based affine interpolant from* x_0 *to* x_T *is given by:*

$$x(t) = R(0, (1 + 4t)\pi/6, \pi/6).$$

Figure 1 shows the curve $t \mapsto x(t)[1\ 0\ 0]^{\mathrm{T}}$ *in the unit 2-sphere* $S^2 \subset E^3$*, which takes the long way round, as does* $t \mapsto x(t)[0\ 1\ 0]^{\mathrm{T}}$*. So with chart-based interpolation, nearby points in SO*(3) *are not always interpolated by nearby curves.* □

When these kinds of situations are avoided by using numerous small charts, we find other difficulties with chart-based interpolants. When x_0 and x_T lie in the intersection of two charts a choice has to be made between two (usually distinct) chart-based interpolants.

Definition 1. *Let* $x : [0, 1] \to Z$ *and* $y : [0, 1] \to Z$ *be continuous curves in a topological space Z. When* $x(1) = y(0)$ *the* track-sum $x.y : [0, 1] \to Z$ *of x and y is defined by* $(x.y)(t) := x(2t)$ *or* $(x.y)(t) := y(2t - 1)$ *accordingly as* $t \in [0, 1/2]$ *or* $t \in [1/2, 1]$. □

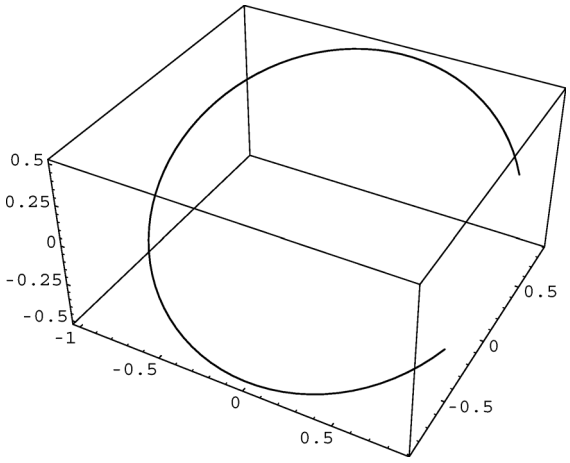


Fig. 1. First column of the chart-based interpolant in Example 1.

Of course track-summation is not commutative, nor even associative. The term "track-sum" is sometimes applied to reparameterisations of track-sums in the sense of Definition 1.

When x_0 and x_T lie in different charts they have to be interpolated by a track-sum of curves with junctions somehow chosen in intersections of overlapping charts. If a differentiable interpolant is required then smoothing has to be carried out near junctions. So there are arbitrary choices, quite a lot of book-keeping, and finally an interpolant that is still not very well-behaved. For instance the interpolant from x_T to x_0 is unlikely to be the reverse of the interpolant from x_0 to x_T. All these difficulties are traceable to a failure to properly account for the geometry of $SO(3)$.

1.2. Quaternions and Spheres

At least locally, the three-manifold $SO(3)$ resembles the unit 3-sphere S^3 in Euclidean 4-space E^4. This can be seen using the quaternion algebra H, as we summarise pp. 265, 266 from ref. [39]:

Because H and E^4 are isometric as real vector spaces, unit quaternions can be identified with points in S^3. Then, for $q \in S^3$, the linear transformation $R(q) : E^4 \cong H \to H \cong E^4$ given by:

$$R(q)r := qr\bar{q} \quad \text{for } r \in H \cong E^4$$

lies in $SO(3)$, where $\bar{q}$ denotes the quaternionic conjugate of $q \in S^3$. Indeed, $R : S^3 \to SO(3)$ is a double cover and, by requiring R to be a local isometry, the standard Riemannian metric on S^3 induces a bi-invariant Riemannian metric on the Lie group $SO(3)$. Another way to say this is that $SO(3)$ is isometric with *real projective* 3*-space*.

So if we could interpolate in S^3, Problem 1 could also be solved as follows:

- Given $x_0, x_T \in SO(3)$ write $x_0 = R(\pm\tilde{x}_0)$, $x_T = R(\pm\tilde{x}_T)$.
- Using the double-cover R, map the four interpolants in S^3 from $\pm\tilde{x}_0$ to $\pm\tilde{x}_T$ to curves in $SO(3)$. Of these four interpolants in $SO(3)$ from x_0 to x_T, choose the one that is best according to some performance measurement. For instance the shortest curve can be found by applying R to only two interpolants in S^3, from x_0 to $\pm x_T$.

This raises the question of how to interpolate in S^3. Thinking of S^3 as a three-dimensional version of the familiar unit 2-sphere S^2 in E^3, there are some obvious things to try.

Method 2. *Given* $\tilde{x}_0, \tilde{x}_T \in S^3$ *the line*

$$t \mapsto \hat{x}(t) := (1 - t/T)\tilde{x}_0 + (t/T)\tilde{x}_T \in E^4$$

does not intersect S^3 *at any other point. If* $\tilde{x}_0 = \tilde{x}_T$ *we would surely take x to be constant. If* $\tilde{x}_0 \neq \pm\tilde{x}_T$ *we might try the*

https://doi.org/10.1017/S0263574707003669 Published online by Cambridge University Press

normalised affine line:

$$\tilde{x}(t) := \frac{\hat{x}(t)}{\|\hat{x}(t)\|} \in S^3$$

which is well-defined and C^∞, because the denominator is never zero. The exceptional case $\tilde{x}_0 = -\tilde{x}_T$ is problematic for any method, and we ignore it. □

Normalised affine lines are much better than chart-based interpolants, but they have (sometimes very) variable speeds, especially when $\tilde{x}_0$ and $\tilde{x}_T$ are nearly antipodal. This seems unreasonable when we are just interpolating between two given data points, and is a serious difficulty in applications requiring estimation of angular velocities. For the interpolation problem in $SO(3)$ the worst extremes can be avoided by choosing $\tilde{x}_0, \tilde{x}_T$ to lie in the same hemisphere but, even so, the interpolants have significantly variable speeds.

Example 2. *Take $\tilde{x}_0 = (0, 1, 0, 0)$, $\tilde{x}_T = (1, 0, 0, 0)$, and $T = 1$. Then:*

$$\|\dot{\tilde{x}}(t)\| = \frac{1}{1 - 2t + 2t^2}$$

with minimum value 1 at $t = 0, 1$, and maximum 2 at $t = 1/2$. □

The cure is to reparameterise $\tilde{x}$ to a curve of constant speed, but this gives us nothing more than a complicated way of arriving at the elementary geometrical notion of a *minimal geodesic* in S^3.

Method 3. *A* minimal geodesic arc *in S^3 is a constant-speed shortest great-circle arc. For $\tilde{x}_0 \neq -\tilde{x}_T$ there is a unique minimal geodesic arc from $\tilde{x}_0$ to $\tilde{x}_T$. The minimal geodesic arc is the constant-speed curve of least length from $\tilde{x}_0$ to $\tilde{x}_T$, and this property is used to define geodesics in other manifolds. In particular the local isometry R maps constant-speed great circle arcs in the same hemisphere of S^3 to minimal geodesic arcs in $SO(3)$.*

More generally, a smooth manifold M is Riemannian *when each tangent space TM_y is equipped with an inner product $\langle , \rangle_y$ depending smoothly on $y \in M$. The Riemannian* length *of a piecewise-C^1 curve $x : [0, T] \to M$ is defined as:*

$$\int_0^T \|\dot{x}(t)\|_{x(t)}\, dt$$

where $\| \|_y$ is the norm on TM_y associated with $\langle , \rangle_y$. Minimal geodesics are defined as constant-speed curves of minimum Riemannian length with given endpoints. Minimal geodesics also minimise the Riemannian energy:

$$J_1(x) := \int_0^T \|\dot{x}(t)\|^2_{x(t)}\, dt \qquad (1)$$

over all curves x (constant-speed or not) with given endpoints. A very good introduction to Riemannian geometry can be found in Parts II and III of the monograph by Milnor.[40] □

Minimal geodesic interpolation is the natural extension of affine interpolation in E^3 to interpolation in S^3 or $SO(3)$. It is easy to implement, quick (around half as fast for $SO(3)$ as for S^3), and gives a generally well-behaved solution to our test problem. Minimal geodesic arcs are constant-speed and do not stray unnecessarily from endpoints (nearby points are interpolated by nearby curves). However Problem 1 is far too elementary for a solution to be useful in applications. What would we do if x or its derivatives were specified at more than two times t_i? If $x(t_i)$ were specified at $t_0 < t_1 < \cdots < t_n$ with $n > 1$ we might choose x to be *piecewise-geodesic*. Just like piecewise-affine interpolants in E^3, piecewise-minimal geodesic interpolants have advantages of simplicity and robustness. However, they are usually not differentiable at the junctions t_i for $0 < i < n$, which is a disadvantage in applications, especially for estimating angular velocity.

1.3. Higher order interpolants

In classical approximation theory, good rates of approximation to differentiable curves are achieved by using *higher order* (not piecewise-affine) curves, especially splines (piecewise-polynomial or piecewise-rational curves). For instance, consider:

Problem 2. *For $t_0 < t_1 < \cdots < t_n$ with $n \geq 1$, let $x_0, x_1, \ldots, x_n \in E^m$ be given together with $v_0, v_n \in E^m$. How should we choose an interpolant $x : [t_0, t_n] \to E^m$ so that $x(t_i) = x_i$ for all $i = 0, 1, \ldots n$ with $\dot{x}(t_0) = v_0$ and $\dot{x}(t_n) = v_n$?* □

The C^2 cubic polynomial spline with knots t_i is a good solution to Problem 2. In particular, when $n = 1$ we would probably choose the cubic polynomial interpolant. The more general problem, where $n = 1$ and M is a Riemannian manifold, is much less straightforward:

Problem 3. *For $T > 0$ let x_0, x_T be given points in a Riemannian manifold M, together with $v_0 \in TM_{x_0}$ and $v_T \in TM_{x_T}$. How should we choose an interpolant $x : [0, T] \to M$ so that $x(0) = x_0, x(T) = x_T, \dot{x}(0) = v_0$ and $\dot{x}(T) = v_T$?* □

Most Riemannian manifolds contain no polynomial curves and, whereas geodesics are natural generalisations of affine lines, there are many more possibilities when it comes to generalising polynomials of degree greater than 1. There is no single class of curves in a Riemannian manifold generalising cubic polynomials in M but, following the pattern of discussion in Sections 1.1 and 1.2, there are some simple things we can try in connection with Problem 3.

Method 4. *With luck, x_0, x_T lie in a common coordinate chart of our manifold M. Then the chart diffeomorphism maps x_0, x_T to points in an open subset of E^m. Similarly, the derivatives of the chart diffeomorphism map v_0, v_T to vectors in E^m. This data can be interpolated by a cubic polynomial in E^m, and if our luck holds the cubic remains within the image of the chart diffeomorphism. Then the corresponding curve in M is our chart-based cubic interpolant. As might be expected, these curves are as badly behaved in every respect as the chart-based affine interpolants of Section 1.1. Notice that the Riemannian structure is not used in the construction of chart-based affine curves or cubics, although it might enter indirectly via chart diffeomorphisms, as in ref. [29].* □

Method 5. *For $M = S^m$ we can take advantage of the embedding of S^m in Euclidean $m + 1$-space E^{m+1}. More precisely,*

https://doi.org/10.1017/S0263574707003669 Published online by Cambridge University Press

since x_0, x_T, v_0, v_T can be regarded as points in E^{m+1}, a cubic polynomial $\tilde{x} : [0, T] \to E^{m+1}$ solves Problem 3 with M replaced by E^{m+1}. With luck, $\tilde{x}(t)$ is never zero. Then the normalised cubic polynomial $x : [0, T] \to S^m$ defined by:

$$x(t) := \frac{\tilde{x}(t)}{\|\tilde{x}(t)\|}$$

satisfies the constraints of Problem 3. The Riemannian structure of S^m is not used in this construction, which also applies to polynomials of other degrees (indeed to any nowhere-zero curves in E^{m+1}). Unsurprisingly in view of Example 2, normalised polynomials of all degrees can have highly variable speed. There are some related constructions that moderate this defect. □

No single method of generating curves in Riemannian manifolds has all the useful properties of polynomials in Euclidean spaces. Rather, depending on what property is emphasised, there are many different families of curves, each with merits and disadvantages. A few examples will have to suffice.

Method 6. *A never-zero polynomial curve (indeed any never-zero curve) in E^{m+1} defines a curve in real projective m-space, whose points are given by homogenous coordinates in $E^{m+1} \setminus \{\mathbf{0}\}$. This gives algebraically defined curves in projective spaces ($m = 3$ for SO(3)) and spheres, along the lines of ref. [20] and [37] by Dietz, Hoschek and Jüttler. This is a more elegant construction than Method 5 but, for a widely spaced data, it is susceptible to the same kinds of difficulties.* □

Method 7. *Working in S^m, S. Buss and J. Fillmore[8] define analogues of B-spline curves by replacing weighted sums of B-spline control vertices by* spherical weighted averages, *namely $x(t)$ is defined as the minimiser of $\sum B_j(t) d(y, p_j)^2$. Here the B_j are B-spline basis functions, the $p_j \in S^m$ are control vertices, d denotes spherical distance, and the minimum is taken over all $y \in S^m$. So each time $x(t)$ is calculated we must solve a nonlinear optimisation problem. Replacing d by Riemannian distance, Buss–Fillmore curves can be defined in the same way in any Riemannian manifold. A detailed discussion of the literature can also be found in ref. [8].* □

Many other methods can be described under two general headings: geometrical constructions and variational curves.

2. Part II: Geometrical Constructions

2.1. Generalised de Castlejau algorithm

As seen in Sectioon 1.2, minimal geodesics in (standard) S^3, and (bi-invariant) $SO(3)$, are readily computed. The same holds for some other Riemannian metrics of interest in applications, and for other homogeneous spaces of Lie groups. However, as noted in the last paragraph of Section 1.2, piecewise-minimal geodesic interpolation is too crude for most applications. Richer classes of curves are needed, resembling polynomials in E^m. A polynomial curve in E^m can be written as $x(t) = \sum_{k=0}^{q} c_k t^k$ where $c_0, c_1, \ldots c_q \in E^m$ and $t \in \mathbb{R}$. However, this is not the only way to write it, nor even the best way, from the point of view of the classical approximation theory.

Definition 2. *For $p_0, p_1 \in E^m$ and $t \in [0, 1]$ set $\beta_1(t, p_0, p_1) := (1 - t)p_0 + tp_1 \in E^m$, namely $\beta_1(t, p_0, p_1)$ divides the line segment from p_0 to p_1 in the ratio $t : 1 - t$.* □

For $p_0, \ldots, p_q \in E^m$ with $q > 1$, the *de Castlejau algorithm* defines $\beta_q(t, p_0, \ldots, p_q) \in E^m$ inductively by

$$\beta_q(t, p_0, \ldots p_q) := \beta_1(t, \beta_{k-1}(t, p_0, \ldots p_{q-1}), \beta_{k-1}(p_1, \ldots, p_q)).$$

Then $x(t) := \beta_q(t, p_0, \ldots, p_q)$ is a (Bézier) polynomial of degree at most q, specified by *control vertices* $p_0, \ldots, p_q$ instead of coefficients c_k. All polynomial curves can be written this way.

K. Shoemake[65] and T. Duff[22] use an adapted de Castlejau algorithm to define the curves in S^3 and $SO(3)$. As noted in,[55] the construction extends in the same way to define generalised Bézier curves in arbitrary Riemannian manifolds, with a single modification: replace line segments by minimal geodesic arcs in Definition 2. It helps if the manifold is *complete* because then any two points are joined by a minimal geodesic. Even when M is complete, the minimal geodesic arc $t \mapsto \beta(t, p_0, p_1)$ can fail to be uniquely defined for some choices of p_0, p_1, as happens when $M = S^m$ with standard metric and $p_0 = -p_1$.

In ref. [65] Shoemake shows how to piece together generalised degree 3 Bézier curves in S^3 into C^1 curves with uniformly spaced knots (uniform splines).

Definition 3. *The* control polygon *of a $q + 1$-tuple of points $p_k \in E^m$ is the piecewise-affine curve $\bar{p} : [0, 1] \to E^m$ given by $\bar{p}(t) := \beta_1(qt - k, p_k, p_{k+1})$ for $t \in [k/q, (k + 1)/q]$ where $k = 0, \ldots q - 1$.* □

Unlike splines in E^3, the control polygons for Shoemake splines in S^3 are not so easy to visualise. So, ref. [43] aims to construct optimal control polygons for these kinds of splines:

Problem 4. *If $n + 1$ given points in S^m are to be interpolated by a C^1 uniform spline consisting of n generalised Bezier curves of degree 2, how should the control points be chosen?* □

Only one control point can be freely prescribed, with the others determined by the interpolation condition and the condition that the spline be C^1. Two critera for optimality are studied in ref. [43]. In ref. [25], Q. Ge and B. Ravani investigate generalised Bézier curves in the group $SE(3)$ of Euclidean motions, deriving a formula for endpoint velocities and a recursive formula for endpoint accelerations. These results and others in ref. [1] can be rewritten as similar statements for S^3. In ref. [16], P. Crouch *et al.* derive explicit formulae for endpoint velocities and covariant accelerations of generalised Bézier curves, and for control points in terms of these quantities, when M is a compact Lie group with bi-invariant Riemannian metric. They also construct generalised Bézier curves of degree 3 with specified endpoint velocities and covariant accelerations when $M = S^m$. These results

https://doi.org/10.1017/S0263574707003669 Published online by Cambridge University Press

permit generalised Bézier curves in compact Lie groups and spheres to be pieced together into C^2 splines.

In ref. [60], the authors compute endpoint velocities and covariant accelerations for generalised Bézier curves of arbitrary degree in S^m. The formulae involve only vector additions, inner products and trigonometric functions (comparing favourably with previous formulae in ref. [16] using exponentials of skew-symmetric matrices). For uniform generalised Bézier splines, ref. [60] extends Shoemake's condition for C^1 continuity to a condition for C^2 continuity (a simple relationship between control points of neighbouring generalised Bézier segments). Results in ref. [60] are extended in ref. [61] to give the formulae for endpoint velocities and covariant accelerations of generalised Bézier curves in a very general class of Riemannian manifolds M. Also in ref. [61], the construction of C^2 uniform generalised Bézier splines in ref. [60] is extended from spheres to symmetric spaces: in particular, M can be an arbitrary Lie group with bi-invariant Riemannian metric.

2.2. Recursive subdivision

The *subdivision property* of Bézier curves in E^m is important in computer graphics:

Property 1. *Given* $p_0, \ldots p_q \in E^m$ *and* $u \in [0, 1]$ *set* $p := (p_0, \ldots, p_q)$ *and define* $q+1$*-tuples* $L(u, p)$, $R(u, p)$ *of control points in* E^m *by*:

- $L(u, p)_0 := p_0$ *and* $L(u, p)_k := \beta_k(u, p_0, \ldots, p_k)$ *for* $k = 1, \ldots, q$.
- $R(u, p)_q := p_q$ *and* $R(u, p)_k := \beta_{q-k}(u, p_k, \ldots, p_q)$ *for* $k = 0, \ldots q-1$.

Then $\beta_q(t, p) = \beta_q(t/u, L(u, p))$ *or* $\beta_q(t, p) = \beta_q((t-u)/(1-u), R(u, p))$, *according as* $t \in [0, u]$ *or* $t \in [u, 1]$. □

Using the subdivision property and the fact that a Bézier curve in E^m is contained in the convex hull of its control vetrices, J. Lane and R. Riesenfeld introduced a *recursive subdivision scheme* for the numerical evaluation of Bézier curves[38] as follows:

Method 8. *Given* $p_0, \ldots, p_q$

- *Set* $p^L := L(1/2, p)$ *and* $p^R := R(1/2, p)$
- *Repeat, with* p^L *in place of* p, *then with* p^R *in place of* p, *and repeat* ...

This gives:

$$p^L, p^R$$
$$p^{LL}, p^{LR}, p^{RL}, p^{RR}$$
$$p^{LLL}, p^{LLR}, p^{LRL}, p^{LRR}, p^{RLL}, p^{RLR}, p^{RRL}, p^{RRR}$$

and so on. Denote the track-sum of the control polygons on the nth line by p^n. *Then the* p^n *converge uniformly (and rapidly) to* $t \mapsto \beta_q(t, p)$. □

Method 8 adapts in the same way as the de Castlejau algorithm defining curves in any complete Riemannian manifold M. However, as noted in ref. [25], generalised Bézier curves do not satisfy the subdivision property. So, unlike the Euclidean case, there is no reason to believe that the Riemannian version of Method 8 will give generalised Bézier curves. Indeed, whereas generalised Bézier curves are C^∞, curves produced by Method 8 in a Riemannian manifold are:

- C^1 with Lipschitz derivatives for $q = 2, 3$ (see ref. [44], [45])
- Usually not everywhere C^2, for $q = 2$ (see ref. [46])
- C^2 on the complement of a countable dense subset of $[0, 1]$, for $q = 2$ (see ref. [46])

Some interpolation properties for $q = 2$ are established in ref. [47].

2.3. Generalised B-spline curves

The Cox-de Boor algorithm[13,18] is a geometrical method for constructing (piecewise-polynomial) B-spline curves in E^m. At each step, $\beta_1(u, v, w)$ is calculated for some $v, w \in E^m$ and some ratio $u \in [0, 1]$. For v, w in a complete Riemannian manifold M, we interpret $\beta(u, v, w)$ as the point dividing a minimal geodesic from v to w in the ratio $u : 1-u$. Then the *generalised Cox-de Boor algorithm* gives *generalised B-spline curves* in M.[21,23,41,42,66] Unlike B-spline curves in E^m, a generalised B-spline curve of degree q may fail to be C^{q-j} at a knot of multiplicity j.[34] In ref. [63], the second author proves that generalised B-spline curves of degree q are C^1 at knots of multiplicity $\leq q-1$, and also computes the (usually non-zero) difference between left and right covariant accelerations at knots of multiplicity $\leq q-2$. Generalisations of recursive algorithms for B-splines are studied in refs. [57], [67] and [68]. Wallner and Dyn show that generalised recursive uniform B-splines are C^1.[68] In ref. [67], Wallner shows that these curves are C^2 provided the degree is greater than 2.

3. Part III: Variational Curves

3.1. Riemannian cubics

For piecewise-C^2 curves x satisfying the interpolation constraints of Problem 2 in Section 1.2,

$$J_2(x) := \int_{t_0}^{t_n} \|\ddot{x}(t)\|^2 \, dt \tag{2}$$

is minimised by the interpolating C^2 cubic spline x with knots $t_0, \ldots t_n$. As seen in Section 1.2, the Riemannian analogues of line segments are minimal geodesics, namely minimisers of the Riemannian quantity J_1. *Riemannian cubic splines* are defined as extremals of a Riemannian analogue of J_2. To say precisely what this means takes more than replacing $\|\|$ by $\|\|_{x(t)}$ in Eq. (2). The difficulty is that whereas $\dot{x}(t)$ is a well-defined vector in the tangent space $TM_{x(t)}$, the *second* derivative $\ddot{x}(t)$ of a C^2 curve x in a Riemannian manifold is generally[1] *undefined*. The standard fix is to replace $\ddot{x}(t)$ by the *covariant derivative* of the vector field $t \mapsto \dot{x}(t)$ defined along x. There are continuously many covariant derivatives, but precisely one that is geometrically compatible with a given Riemannian structure, namely the

[1] As seen in Section 3.5.3 it is a different story when M is equipped with a smooth embedding in a Euclidean space.

https://doi.org/10.1017/S0263574707003669 Published online by Cambridge University Press

Levi-Civita covariant derivative ∇. For present purposes it suffices to define ∇ for $M = S^m$ with the standard Riemannian metric:

Definition 4. *Let* $x : \mathbb{R} \to S^m$ *be at least* C^1. *Let*

$$y \mapsto Y_y \in TS^m_y = \{v \in E^{m+1} : \langle v, y\rangle = 0\}$$

be a C^1 *vector field defined at least along the image of* x. *Then* $t \mapsto Y_{x(t)} \in TS^m_{x(t)} \in E^{m+1}$ *defines a* C^1 *function* $f : \mathbb{R} \to E^{m+1}$. *It happens that usually* $\dot f(t) \notin T S^m_{x(t)}$, *and so* $\dot f$ *does not define a vector field along* x. *This defect is easily fixed by projecting orthogonally onto tangent spaces, namely:*

$$\nabla_{d/dt} Y := \dot f(t) - \langle \dot f(t), x(t)\rangle x(t) \in TS^m_{x(t)}. \qquad \square$$

Then the (Levi-Civita) *covariant acceleration* $\nabla_{d/dt}\dot x(t)$ is a vector field defined along x, and

$$J_2(x) := \int_{t_0}^{t_n} \left\|\nabla_{d/dt}\dot x(t)\right\|^2_{x(t)}\, dt \tag{3}$$

is defined for any piecewise-C^2 curve $x : \mathbb{R} \to M$. A *Riemannian cubic* is an extremal of J_2 for Problem 3 (the 2-point problem of Section 3). Riemannian cubic splines are C^2 track-sums of Riemannian cubics as proved in ref. [14].

Riemannian cubics were introduced by Gabriel and Kajiya[24] and independently by Heinzinger *et al.*[48] In these papers, the Euler Lagrange equation for a Riemannian cubic $x : \mathbb{R} \to M$ in a Riemannian[2] manifold M is proved to be:

$$\nabla^3_{d/dt}\dot x(t) + R_{x(t)}\big(\nabla_{d/dt}\dot x(t), \dot x(t)\big)\dot x(t) = \mathbf{0} \tag{4}$$

where the *Riemannian curvature* tensor field R is defined according to the convention:

$$R(X, Y)Z := \nabla_X\nabla_Y Z - \nabla_Y\nabla_X Z - \nabla_{[X,Y]}Z$$

for C^2 vector fields X, Y, Z on M, and $[\ ,\ ]$ denotes the *Lie bracket*.[30]

Example 3. *For* $M = E^m$ *with the Euclidean metric, the curvature term vanishes and Eq. (4) reduces to* $x^{(4)}(t) = 0$. *This is consistent with the result, from classical approximation theory, that cubic polynomials in* E^m *minimise* J_2.[19] $\square$

In general, Eq. (4) is equivalent in each coordinate chart to a complicated fourth-order system of nonlinear ODEs for m unknown real-valued functions, rewritable as a first order $4m$-dimensional nonlinear dynamical system.

Example 4. *Figure 2 shows the curve in* S^2 *obtained by taking the last columns of the Riemannian cubic (bold) and the generalised Bézier cubic (light) in* $SO(3)$ *joining*

$$x_{jT} = \begin{bmatrix} 1 & 0 & 0 \\ 0 & \sqrt{3}/2 & (-1)^j/2 \\ 0 & (-1)^{j+1}/2 & \sqrt{3}/2 \end{bmatrix}$$

[2]The proofs work in the same way for any semi-Riemannian manifold M.

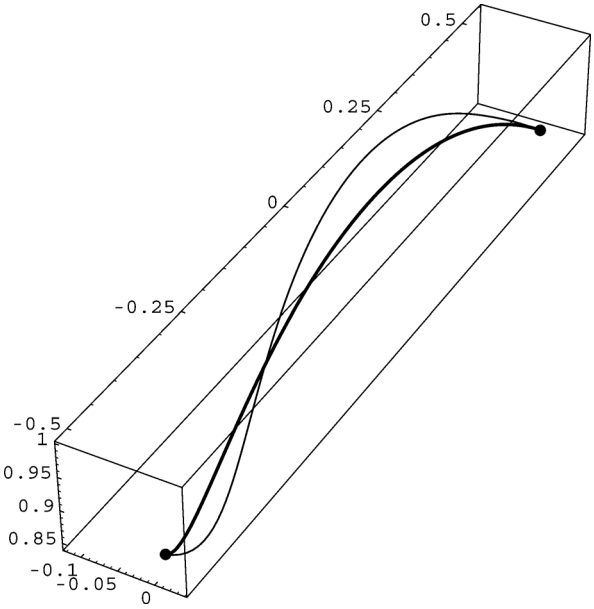


Fig. 2. Projections of the Riemannian (bold) and generalised Bézier cubics in Example 4.

for $j = 0, 1$ *with* v_0 *and* v_T *as*:

$$\begin{bmatrix} 0.0000 & 0.9280 & -0.3725 \\ -0.7175 & -0.1225 & 0.2121 \\ 0.7866 & -0.2121 & -0.1225 \end{bmatrix} \text{ and}$$

$$\begin{bmatrix} 0.0000 & -0.2708 & -0.2380 \\ 0.1155 & -0.0224 & -0.0388 \\ 0.3415 & 0.0388 & -0.0224 \end{bmatrix}$$

respectively. As might be expected, the projection of the Riemannian cubic appears to show less variability. $\square$

In ref. [48], it is shown[3] for Lie groups G with bi-invariant Riemannian metric that Eq. (4) is equivalent to the system

$$\dot x(t) = (dL(x(t)))_e(V(t)) \tag{5}$$

$$\dot V(t) = [\dot V(t), V(t)] + C \tag{6}$$

where $L(y)$ denotes left-multiplication by $y \in G$, e is the identity of G, V is a curve (the *Lie quadratic* of x) in the Lie algebra $\mathcal{G} = TG_e$ of G, and $C \in \mathcal{G}$ is constant. For a matrix group G, Eq. (5) can be viewed as a linear equation for x with variable coefficients V. In ref. [53], Eq. (5) is solved by quadratures in terms of V for generic cases where G is semi-simple. In ref. [52], elementary and explicit constructions are given for $SO(3)$ and $SO(1, 2)$.

Equation (6) is a second-order analogue of the Euler equation for the motion of a (spherically symmetric unforced) rigid body, as in Theorem 13.8.3 of ref. [39]. Note that V is a curve in a real vector space $\mathcal{G}$, whereas x is a curve in a Lie group. Moreover, when G is $SO(3)$ or S^3, there is a

[3]The proof given for $G = SO(3)$ adapts readily.

https://doi.org/10.1017/S0263574707003669 Published online by Cambridge University Press

Lie-isomorphism $(\mathcal{G}, [\ ,\ ]) \cong (E^3, \times)$ where $\times$ is the cross-product. So for $SO(3)$ and S^3, Lie quadratics can be identified with curves in E^3 satisfying

$$\ddot{V}(t) = \dot{V}(t) \times V(t) + C \tag{7}$$

where $C \in E^3$ is constant. When $C = 0$ the Lie quadratic V is said to be *null*.

Example 5. *For $b_0, b_1 \in E^3$ the affine function $t \mapsto b_0 + tb_1$ is a Lie quadratic, and it is null when b_0, b_1 are linearly dependent. The affine Lie quadratics are the only examples for which quadrature solutions of Eq. (5) are not given in ref. [52]. Asymptotic dynamics of a spherically symmetric ball under a torque constant in body coordinates, and of a rolling ball on an inclined plane, can be determined using properties of nonaffine null Lie quadratics (Theorem 1 below).* □

Example 6.[50] *Given $a_0, c_0, t_0 \in \mathbb{R}$ and $A \in SO(3)$, define*

$$V(t) := a_0 A(-c_0, \cos(a_0 c_0(t - t_0)), \sin(a_0 c_0(t - t_0))).$$

Then V is a Lie quadratic with $C = a_0^3 c_0 A(1, 0, 0)$. □

These are the only examples where Lie quadratics can be written down explicitly. Methods for approximate solution of Eqs. (5) and (6) are given in ref. [56]. Alternatively, a discrete analogue of J_2 can be minimised subject to the interpolation constraints.[2]

3.2. Null Lie quadratics in E^3

In ref. [49], nonconstant null Lie quadratics in E^3 are shown to have constant curvature, linear torsion, internal symmetry and asymptotic *axes*

$$\alpha_\pm := \lim_{t \to \pm\infty} \frac{V(t)}{\|V(t)\|}.$$

The study of null Lie quadratics reduces to the case where V is *canonical*, namely $\|\dot{V}(0)\| = 1$ and $\langle V(0), \dot{V}(0)\rangle = 0$.

Example 7. *Taking $V(0) = (1.5, 0, 0)$, $\dot{V}(0) = (0, 1, 0)$, $C = (0, 0, 0)$ and solving Eq. (7) numerically for $t \in (-12, 12)$ we obtain the canonical null Lie quadratic shown in Fig. 3. By Eqs. (14) and (15) of ref. [49], V has constant curvature $3/2$, and torsion $\tau(t) = -t$ that is linear in the parameter t (we would not guess these facts from Fig. 3). Theorem 4 of ref. [49] asserts symmetry of the image of V about the plane through $(3/2, 0, 0)$ orthogonal to $(0, 1, 0)$, which can be seen in our illustration, as well as existence of asymptotic axes*

$$\alpha_\pm \approx (0.891427, \pm 0.17092, -0.419696)$$

□

Taking $C = 0$ in Eq. (7), $\langle \ddot{V}(t), V(t)\rangle$ and $\langle \ddot{V}(t), \dot{V}(t)\rangle$ are identically 0. Also, as noted in ref. [49], canonical null Lie quadratics in E^3 satisfy

$$\|V(t)\|^2 = t^2 + c$$
$$\|\dot{V}(t)\| = 1$$
$$\|\ddot{V}(t)\|^2 = c$$

for all $t \in \mathbb{R}$ where $c \geq 0$ is constant. When $c = 0$ V is affine. For $c > 0$ there have been some recent results on asymptotic properties of canonical null Lie quadratics V in E^3 with $c > 0$:

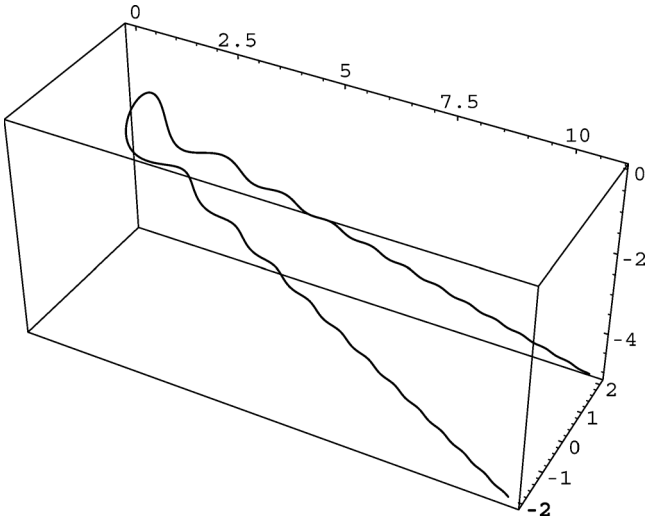


Fig. 3. Canonical null Lie quadratic in Example 7.

Theorem 1.[54] *For some $\beta_\pm \in S^2$ with $\langle \alpha_\pm, \beta_\pm\rangle = 0$ we have, as $t \to \pm\infty$,*

$$V(t) = f(t)\alpha_\pm - \frac{\sqrt{c}}{f(t)^2} \exp(\mp g(t) I_\pm)\beta_\pm + O\left(\frac{1}{f(t)^3}\right)$$
$$\dot{V}(t) = \frac{t}{f(t)}\alpha_\pm + \frac{\sqrt{c}}{f(t)} I_\pm \exp(\mp g(t) I_\pm)\beta_\pm + O\left(\frac{1}{f(t)^2}\right)$$
$$\ddot{V}(t) = \sqrt{c} \exp(\mp g(t) I_\pm)\beta_\pm + O\left(\frac{1}{f(t)}\right)$$

where $f(t) := \sqrt{t^2 + c}$, $g(t) := \frac{1}{2}(tf(t) + c \ln(t + f(t))) - (c/2)\ln c$, and $I_\pm$ is the linear automorphism of $\alpha_\pm^\perp := \{v \in E^3 : \langle \alpha_\pm, v\rangle = 0\} \subset E^3$ given by $I_\pm v := \alpha_\pm \times v$. □

3.3. Non-null Lie quadratics

Non-null Lie quadratics are only occasionally affine or periodic, as in Examples 5, 6, and frequently exhibit much more complicated dynamics than null Lie quadratics.

Example 8. *Figure 4 shows a numerical solution of (6) for $V : [-45, 30] \to E^3$ where $V(0) = (1, 2, 2)$, $\dot{V}(0) = (-1, 1, 1)$ and $C = -(2/5, 1/2, 3/4)$. After numerous attempts to find axes, the non-null Lie quadratic finally spirals outwards along an asymptotic axis. This behaviour can be seen a little more clearly in Fig. 5 where $U(t) := V(t)/\|V(t)\|$ is plotted over the larger domain $[-240, 30]$, together with*

https://doi.org/10.1017/S0263574707003669 Published online by Cambridge University Press

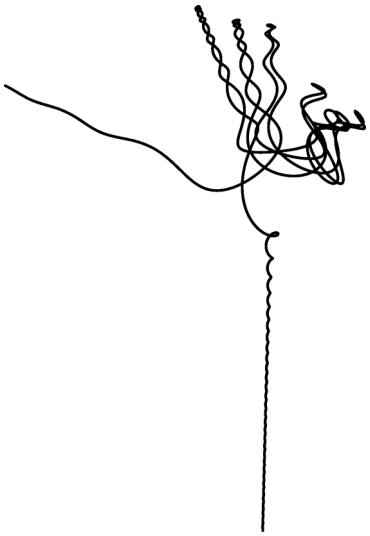


Fig. 4. Non-null Lie quadratic $V : [-45, 30] \to E^3$ in Example 8.

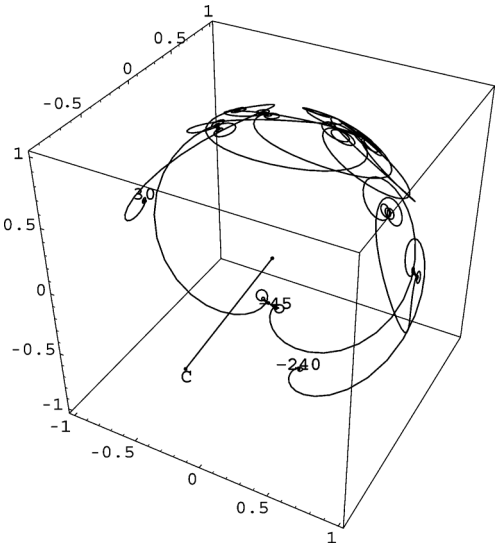


Fig. 5. $U : [-45, 240] \to S^2$ in Example 8.

the line-segment from 0 *to* C. *The points* $U(t)$ *where* $t = -240, -45, 30$ *are labelled.* □

Let V be a non-null Lie quadratic in E^3. By Theorem 1 of ref. [50], $F(t) := \langle V(t), V(t)\rangle$ satisfies

$$F^{(4)}(t) + (\ddot{F}(t) + b)F(t) - \frac{3}{4}\dot{F}(t)^2 = d \qquad (8)$$

for real constants b, d. Other more complicated differential equations and inequalities are also proved, including a nonlinear third-order ODE for F with 17 terms. These are used to prove that all solutions of Eq. (6), whether null or not, extend to Lie quadratics on the whole of $\mathbb{R}$. Asymptotic properties of non-null Lie quadratics are then established, including the existence of asymptotic axes in many cases, and results on rates of growth, the simplest of which is:

Theorem 2. *(Theorem 3 of ref. [30]) If* $b < 0$ *then* F *is strictly convex and* $\liminf_{t\to\pm\infty} \frac{F(t)}{t^4} > 0$. □

Asymptotic results for Lie quadratics imply asymptotic results for Riemannian cubics.[40]

3.4. Other Riemannian manifolds

In addition to $SO(3)$, work has been done on Riemannian cubics in other Riemannian and semi-Riemannian manifolds, notably spheres,[36] $SO(1, 2)$,[52] general semisimple Lie groups,[53] general locally symmetric spaces,[49] complete Riemannian manifolds,[26] and Riemannian manifolds in general.[10] For instance:

- There are relationships between non-null Lie quadratics in E^3 and envelopes of Riemannian cubics in the projective plane[36]
- If x is a Riemannian cubic in a locally symmetric space M, then

$$\left\|\nabla^2_{d/dt}\dot{x}(t)\right\|^2_{x(t)} + \left\langle R_{x(t)}\left(\nabla_{d/dt}\dot{x}(t), \dot{x}(t)\right)\dot{x}(t), \nabla_{d/dt}\dot{x}(t)\right\rangle_{x(t)}$$

  is conserved in t[49]
- R. Giambo *et al.*[26] use critical-point theory on infinite-dimensional manifolds to prove the existence of a global minimiser of J_2 and prove the results on numbers of Riemannian cubics solving Problem 3
- If x is a Riemannian cubic in a general Riemannian manifold then

$$\frac{1}{2}\left\|\nabla_{d/dt}\dot{x}(t)\right\|^2_{x(t)} - \left\langle\nabla^2_{d/dt}\dot{x}(t), \dot{x}(t)\right\rangle_{x(t)}$$

  is conserved in t.[10]

3.4.1. Euclidean motions. The six-dimensional Lie group of Euclidean motions:

$$SE(3) := \left\{\begin{bmatrix} x & y \\ 0 & 1 \end{bmatrix} : x \in SO(3), \quad y \in E^3\right\} \qquad (9)$$

is the configuration space of a rigid body with an orthonormal frame x whose origin of coordinates moves with y.

The parameterisation (Eq. (9)) of $SE(3)$ by $SO(3) \oplus E^3$ (not a group isomorphism) gives left invariant Riemannian metrics on $SE(3)$ using bi-invariant metrics on $SO(3)$ and E^3. Then Riemannian cubics in $SE(3)$ correspond precisely to pairs (x, y) where x is a Riemannian cubic in $SO(3)$ and y is a cubic polynomial. So the numerically computed Riemannian cubics of left-invariant $SE(3)$ computed by Belta and Kumar,[3,4] and by Zefran and Kumar[71,72] can be viewed as examples of Riemannian cubics in $SO(3)$ together with cubic polynomials. Computations are also made in refs. [71] and [72] using the bi-invariant semi-Riemannian metric defined by the *Klein form.*[33]

3.4.2. Left-invariant Riemannian metrics on $SO(3)$. Left-invariant Riemannian metrics on $SO(3)$ are of interest in engineering applications. For a Riemannian cubic x in left-invariant $SO(3)$, the curve V defined by Eq. (5) satisfies a complicated third-order differential equation (Section 5.3 of ref. [35]).

3.5. Other kinds of variational curves

3.5.1. Riemannian cubics in tension. Given a positive real constant τ, Silva Leite *et al.*[58,59] consider minimising

$$J_2^\tau(x) := \int_{t_0}^{t_1} \left\|\nabla_{d/dt}\dot{x}(t)\right\|^2_{x(t)} + \tau\|\dot{x}(t)\|^2_{x(t)}\, dt$$

https://doi.org/10.1017/S0263574707003669 Published online by Cambridge University Press

subject to the constraints[4] of Problem 2 applied to curves in a Riemannian manifold M. The critical points are shown to be C^2 and satisfy

$$\nabla^3_{d/dt}\dot{x}(t) + R\big(\nabla_{d/dt}\dot{x}(t), \dot{x}(t)\big)\dot{x}(t) - \tau\nabla_{d/dt}\dot{x}(t) = 0$$

between knots. As shown in ref. [59], when M is a Lie group G with bi-invariant Riemannian metric, the curve V in the Lie algebra $\mathcal{G}$ defined by Eq. (5) satisfies

$$V^{(3)}(t) = [\ddot{V}(t), V(t)] + \tau\dot{V}(t). \tag{10}$$

In ref. [51] the authors rewrite Eq. (10) in the form

$$\ddot{V}(t) = [\dot{V}(t), V(t)] + C \tag{11}$$

where $C \in \mathcal{G}$. When $C = 0$, V is called a *null Lie quadratic in tension*. Asymptotic properties of null Lie quadratics in tension are proved:

- Asymptotic axes exist for V nontrivial.
- Convergence to axes is exponential.
- V has internal symmetry.

3.5.2. Elastica. For applications in rigid body motion planning it may be desirable to minimise J_2 subject to additional constraints. If the vectors v_0, v_T in Problem 3 satisfy $\|v_0\|_{x_0} = \|v_T\|_{x_T}$ then we can consider minimising J_2 subject to the additional constraint that x be constant-speed (without loss $\dot{x}(t)$ is identically 1). The extremals (*elastica*) satisfy

$$\nabla^3_{d/dt}\dot{x}(t) + R\big(\nabla_{d/dt}\dot{x}(t), \dot{x}(t)\big)\dot{x}(t) + \nabla_{d/dt}(\lambda(t)\dot{x}(t)) = 0 \tag{12}$$

for some C^∞ function $\lambda : \mathbb{R} \to \mathbb{R}$. Elastica in S^2 with the standard Riemannian metric are investigated by Brunnett and Crouch[6] and Brunnett *et al.*,[7] who derive a differential equation for the square of the *geodesic curvature* $\|\nabla_{d/dt}\dot{x}(t)\|_{x(t)}$ and solve for x numerically. Jurdjevic[31,32] uses the Hamiltonian formalism to construct by quadratures the *symmetric elastica* in simply-connected two-and three-dimensional spaces of constant sectional curvature: in S^2 these curves coincide with those in refs. [6] and [7]. In ref. [62], the authors study elastica in compact Lie groups G with bi-invariant Riemannian metric. Elastica are proved to be defined on the whole of $\mathbb{R}$. For $G = SO(3)$, Eq. (12) is solved by quadratures.

3.5.3. Extrinsic variational curves. When M is equipped with an embedding in a Euclidean space E^k for some k, a curve x in M can also be regarded as a curve in E^k. Then $\ddot{x}(t) \in E^k$ and

$$J_2^{\text{ext}}(x) := \int_{t_0}^{t_n} \|\ddot{x}(t)\|^2\, dt$$

is well-defined, where $\|\ \|$ now denotes the Euclidean norm on E^k. Similarly for $\tau > 0$ we have

$$J_2^{ext,\tau}(x) := \int_{t_0}^{t_n} \|\ddot{x}(t)\|^2 + \tau\|\dot{x}(t)\|^2\, dt.$$

Then extrinsic analogues of cubics and cubics in tension can be defined, as extremals of J_2^{ext} and $J_2^{\text{ext},\tau}$ where x is constrained to M. These curves are studied in ref. [28].

Example 9. *Let $M = S^3 \subset E^4$. The extrinsic cubics and cubics in tension are different to Riemannian cubics and Riemannian cubics in tension in S^3 with the standard Riemannian metric.* □

3.5.4. Higher order geodesics. Let $q = 3, 4, 5, \ldots$ be given.

Problem 5. *For $t_0 < t_1 < \cdots < t_n$ with $n \geq 1$, let $x_0, x_1, \ldots, x_n \in M$ be given, together with $v_0^k \in TM_{x_0}$ and $v_n^k \in TM_{x_n}$ for all $k = 1, 2, \ldots, q-1$. How should we choose an interpolant $x : [t_0, t_n] \to M$ so that $x(t_i) = x_i$ for all $i = 0, 1, \ldots n$, and*

$$\nabla^{k-1}_{d/dt}\dot{x}(t_0) = v_0^k \quad \textit{and} \quad \nabla^{k-1}_{d/dt}\dot{x}(t_n) = v_n^k$$

for all[5] $k = 1, 2, \ldots q-1$? □

For piecewise-C^∞ curves $x : [t_0, t_n] \to M$ satisfying the interpolation constraints of Problem 5 in Section 1.2, define

$$J_q(x) := \int_{t_0}^{t_1} \left\|\nabla^{q-1}_{d/dt}\dot{x}(t)\right\|^2_{x(t)} dt.$$

In ref. [12], extremals of J_q are shown to be C^{2q-2} and satisfy

$$\nabla^{2q-1}_{d/dt}\dot{x}(t) + \sum_{k=1}^{q-1}(-1)^j R\big(\nabla^{2q-k-2}_{d/dt}\dot{x}(t), \nabla^{k-1}_{d/dt}\dot{x}(t)\big)\dot{x}(t) = 0 \tag{13}$$

on each (t_{i-1}, t_i) for $i = 1, 2, \ldots, n$. In ref. [27], R. Giambo *et al.* also extend their earlier work[26] from the case $q = 3$ to prove the existence of results for extremals of J_q. In Chapter 9 of the second author's thesis,[64] extremals of J_q with $n = 1$ are called *q-geodesics*.[6] These have also been studied (especially when $q = 3$) by Krakowski,[35] Zefran *et al.*[73] and Machado. In Chapter 9 of ref. [64], it is proved that, for a q-geodesic x in a Lie group G with bi-invariant Riemannian metric, the curve V defined by Eq. (5) satisfies a differential equation of order $2q-1$ of *Lax form*

$$\dot{Z}(t) = [Z(t), V(t)]$$

where Z is given in terms of x and the first $2q-2$ covariant derivatives of $\dot{x}$. This differential equation is integrated to an equivalent equation of the order $2q-2$. The Lax equation

[4] Additional constraints are also considered.

[5] $\nabla^0_{d/dt}$ is interpreted as the identity.

[6] A 1-geodesic is just a geodesic. A 2-geodesic is a Riemannian cubic. Our present focus is on $q \geq 3$.

https://doi.org/10.1017/S0263574707003669 Published online by Cambridge University Press

also enables x to be computed from V by quadrature using methods of ref. [53], at least when G is semisimple.

3.6. Conclusion

The need for mathematical solutions to tasks of path-planning for rigid body motion has led to a surprisingly rich body of research on curves in Riemannian manifolds. As a general rule, natural extensions of standard methods from approximation theory behave in unexpected ways, even when applied to curves in Lie groups modelling elementary physical phenomena. Typically non-Euclidean analogues of equivalent classical methods lead to distinct and inequivalent theories in a Riemannian setting.

Most attention has focused on curves in Lie groups, especially the rotation group $SO(3)$, and to a lesser extent the group $SE(3)$ of Euclidean motions. There have also been significant results for curves in more general Lie groups (especially the semisimple case), and some results for homogeneous spaces (especially spheres). There seems to be a lot of scope for further work along these lines.

Current work includes research by Noakes on applications of asymptotics of Riemannian cubics to nonholonomic problems in classical mechanics. There is ongoing work on numerical implementations of Riemannian cubics for engineering problems, and on applications to symplectic integrators (with Marsden, Kobilarov and Bou-Rabee).

References

1. C. Altafini, "The de Castlejau Algorithm on $SE(3)$," **In:** *Nonlinear Control in Year 2000 Lecture Notes in Control and Information Sciences* (A. Isidori, F. Lamnabhi-Lagarrigue and W. Respondek, eds.) **258**, (Springer, Berlin Germany, 2000) pp. 23–34.
2. A. Barr, B. Currin, S. Gabriel and J. Hughes,"Smooth Interpolation of Orientations with Angular Velocity Constraints using Quaternions," *SIGGRAPH Comput. Graph.* **26**, 313–320 (1992).
3. C. Belta and V. Kumar, "On the computation of rigid body motion," *Electron. J. Computat. Kinematics* **2** (2002).
4. C. Belta and V. Kumar, "Euclidean metrics for motion generation on SE(3)," *J. Mech. Eng. Sci. Part C* **216**, 47–60 (2002).
5. A. M. Bloch, J. Baillieul, P. Crouch and J. Marsden, *Nonholonomic Mechanics and Control* (*Interdisciplinary Applied Mathematics*) **24** (Springer, Berlin, Germany, 2003).
6. G. Brunnett and P. Crouch, "Elastic curves on the sphere," *Adv. Comput. Math.* **2**, 23–40 (1994).
7. G. Brunnett, P. Crouch and F. Silva-Leite, "Spline Elements on Spheres," **In:** *Mathematical Methods for Curves and Surfaces* (Vanderbilt University Press, Nashville, TN, 1995) pp. 49–54.
8. S. Buss and J. Fillmore, "Spherical averages and applications to spherical splines and interpolation," *ACM Trans. Graph.* **20**, 95–126 (2001).
9. S. Buss, "Accurate and efficient simulations of rigid body rotations," *J. Comput. Phys.* **164**, 377–406 (2000).
10. M. Camarinha, The Geometry of Cubic Polynomials on Riemannian Manifolds, *Ph.D. Thesis* (Coimbra, Portugal: University of Coimbra, 1996).
11. M. Camarinha, F. Silva Leite and P. Crouch, "On the geometry of Riemannian cubic polynomials," *Differential Geom. Appl.* **15**(2), 107–135 (2001).
12. M. Camarinha, F. Silva Leite and P. Crouch, "Splines of class C^k on non-Euclidean spaces," *IMA J. Math. Control Inf.* **12**(4), 399–410 (1995).
13. M. Cox, "The numerical evaluation of B-splines," *J. IMA* **10**, 134–149 (1972).
14. P. Crouch and F. Silva-Leite, "Geometry and the Dynamic Interpolation Problem," *Proceedings of the American Control Conference,* Boston, U.K. (1991) pp.1131–1136.
15. P. Crouch and F. Silva Leite, "The dynamic interpolation problem: On Riemannian manifolds, Lie groups, and symmetric spaces," *J. Dynam. Control Syst.* **1**(2), 177–202 (1995).
16. P. Crouch, G. Kun and F. Silva Leite, "The de Castlejau algorithm on Lie groups and spheres," *J. Dynam. Control Syst.* **5**(3), 397–429 (1999).
17. F. Silva Leite, M. Camarinha and P. Crouch, "Elastic curves as solutions of Riemannian and sub-Riemannian control problems," *Math. Control Signals Syst.* **13**(2), 140–155 (2000).
18. C. de Boor, "On calculating with B-Splines," *J. Approx. Theory* **6**, 50–62 (1972).
19. C. de Boor, *A Practical Guide to Splines* (Springer, Berlin, Germany, 2001).
20. R. Dietz, J. Hoschek and B. Jüttler, "An algebraic approach to curves and surfaces on the sphere and other quadrics," *Comput. Aided Geometric Design* **10**, 211–229 (1993).
21. R. Ding, "Drawing ruled surfaces using the Dual de Boor algorithm," *Electron. Notes Theoretical Comput. Sci.* **61**, 178–190 (2002).
22. T. Duff, "Quaternion Splines for Animating Orientation," *Proceedings of the USENIX Association 2nd Computer Graphics Workshop*, Monterey, CA (1985) pp. 54–62.
23. T. Duff, "Splines in Animation and Modelling," **In:** *State of the Art in Image Synthesis, SIGGRAPH '86 Course Notes* (ACM Press, New York, 1986).
24. S. Gabriel and J. Kajiya, "Spline Interpolation in Curved Space," **In:** *State of the Art in Image Synthesis, SIGGRAPH '85 Course Notes* (ACM Press, New York, 1985), pp. 1–14.
25. Q. Ge and B. Ravani, "Geometric Construction of Bézier Motions," *Trans. ASME J. Mech. Des.* **116**, 749–755 (1994).
26. R. Giambo, F. Giannoni and P. Piccione, "An analytical theory for Riemannian cubic polynomials," *IMA J. Math. Control Inf.* **19**, 445–460 (2002).
27. R. Giambo, F. Giannoni and P. Piccione, "Optimal control on Riemannian manifolds by interpolation," *Math. Control, Signals Syst.* **16**, 278–296 (2004).
28. M. Hofer and H. Pottmann, "Energy-minimising splines in manifolds," *ACM Trans. Graph.* **23**, 284–293 (2004).
29. K. Hüper and F. Silva-Leite, "On the geometry of rolling and interpolation curves on S^n, SO_n and Grassmann manifolds," *J. Dynam. Control Syst.* (2007) to be published.
30. J. Jost, *Riemannian Geometry and Geometric Analysis* (*Universitext*) (Springer, Berlin, Germany, 1995).
31. V. Jurdjevic, "Non-Euclidean elastica," *Amer. J. Math* **117**, 93–124 (1995).
32. V. Jurdjevic, *Geometric Control Theory (Cambridge Studies in Advanced Mathematics)* **51** (Cambridge University Press, Cambridge, U. K, 1997).
33. A. Karger and J. Novak, *Space Kinematics and Lie Groups* (Gordon and Breach, New York, 1985).
34. M.-J. Kim, M.-S. Kim and S. Shin, "A C^2 Continuous B-Spline Quaternion Curve Interpolating a Given Sequence of Solid Orientations," *Proceedings of the 22nd Annual Conference on Computer Graphics and Interactive Techniques* (1995) pp. 369–376.
35. K. Krakowski, Geometrical Methods of Inference *Ph.D. Thesis* (Perth, Australia: University of Western Australia, 2002).
36. K. Krakowski, "Envelopes of splines in the projective plane," *IMA J. Math. Control Inf.* **22**, 171–180 (2005).
37. B. Jüttler and M. Wagner, "Computer-aided design with spatial rational B-spline motions," *Trans. ASME J. Mech. Des.* **118**, 193–201 (1996).
38. J. Lane and R. Riesenfeld, "A theoretical development for the computer generation and display of piecewise polynomial

https://doi.org/10.1017/S0263574707003669 Published online by Cambridge University Press

surfaces," *IEEE Trans. Pattern Anal. Mach. Intel.* **2**, 35–46 (1980).
39. J. E. Marsden and T. S. Ratiu, *Introduction to Mechanics and Symmetry (Texts in Applied Mathematics)* **17** (Springer, Berlin, Germany, 1994).
40. J. Milnor, *Morse Theory* (*Annals of Mathematical Studies*) **51** (Princeton University Press, NJ, 1963).
41. G. Nielson, "Smooth Interpolation of Orientation," *Proceedings of Computer Animation '93: Models and Techniques in Computer Animation* (1993) pp. 75–93.
42. G. Nielson and R. Heiland, "Animated Rotations using Quaternions and Splines on a 4D Sphere," *Programm. Comput. Softw.* **18**, 145, 154 (1992).
43. L. Noakes, "Spherical Splines," **In:** *Geometric Properties for Incomplete Data* (R. Klette, R. Kozera, L. Noakes, J. Weickert eds.) (*Computational Imaging and Vision)* **31** (Springer, Berlin, Germany, 2006) pp. 77–101.
44. L. Noakes, "Riemannian quadratics," **In:** *Curves and Surfaces with Applications in CAGD* (A. Le Méhauté, C. Rabut and L. Schumaker eds.) (Vanderbilt University Press, Nashville, TN, 1997) pp. 319–328.
45. L. Noakes, "Nonlinear corner-cutting," *Adv. Comput. Math.* **8**, 165–177 (1998).
46. L. Noakes, "Accelerations of Riemannian Quadratics," *Proceedings of the American Mathematical Society* **127** (1999) pp. 1827–1836.
47. L. Noakes, "Quadratic interpolation in spheres," *Adv. Comput. Math.* **17**, 385–395 (2002).
48. L. Noakes, G. Heinzinger and B. Paden, "Cubic splines on curved spaces," *IMA J. Math. Control Inf.* **6**, 465–473 (1989).
49. L. Noakes, "Null cubics and Lie quadratics," *J. Math. Phys.* **44**(3), 1436–1448 (Mar. 2003).
50. L. Noakes, "Non-null Lie quadratics in E^3," *J. Math Phys.* **45**(11), 4334–4351 (2004).
51. L. Noakes and T. Popiel, "Null Riemannian cubics in tension in *SO*(3)," *IMA J. Math. Control Inf.* **22**, 477–488 (2005).
52. L. Noakes, "Duality and Riemannian cubics," *Adv. Comput. Math.* **25**, 195–209 (2006).
53. L. Noakes, "Lax constraints in semisimple Lie groups," Q. J. Math. **57**, 527–538 (2006).
54. L. Noakes, "Asymptotics of null Lie quadratics in E^3," *SIAM J* on Appl. Dyn. Sys. in-press 2007.
55. F. Park and B. Ravani, "Bézier curves on Riemannian manifolds and Lie groups with kinematic applications," *Trans. ASME J. Mech. Des.* **117**, 36–40 (1995).
56. F. Park and B. Ravani, "Smooth invariant interpolations of rotations," *ACM Trans. Graph.* **16**, 277–295 (1997).
57. D. Pletinckx, "Quaternion calculus as a basic tool in computer graphics," *Vis. Comput.* **5**, 2–13 (1989).
58. F. Silva-Leite, M. Camarainha and P. Crouch, "Two Higher Order Variational Problems on Riemannian manifolds and the Interpolation Problem," *Proceedings of the 3rd European Control Conf.* (1995) pp. 3269–3274.
59. F. Silva-Leite, M. Camarainha and P. Crouch, "Elastic curves as solutions of sub-Riemannian control problems," *Math. Control, Signals Syst.* **13**, 140–155 (2000).
60. T. Popiel and L. Noakes, "C^2 spherical Bézier splines," *Comput. Aided Geom. Des.* **23**, 261–275 (2006).
61. T. Popiel and L. Noakes, "Bézier curves and C^2 interpolation in Riemannian manifolds," *J. Approx. Theory* (Oct. 2006) to be published.
62. T. Popiel and L. Noakes, "Elastica in *SO*(3)," *J. Aust. Math. Soc.* (2006) to be published.
63. T. Popiel, "On Parametric Smoothness of Generalised B-Spline Curves," *Comput. Aided Geom. Des.* **23**, 655–668 (2006).
64. T. Popiel, Geometrically Defined Curves in Riemannian Manifolds Ph.D. Thesis (Perth, Australia: University of Western Australia, 2007).
65. K. Shoemake, "Animating rotations with quaternion curves," *SIGGRAPH Comput. Graph.* **19**, 245–254 (1985).
66. K. Sprott and B. Ravani, "Ruled surfaces, Lie groups and mesh generation," *Proceedinds of the ASME Design Engineering Technology Conference* (1997) No. DETC97/DAC-3966.
67. J. Wallner, "Smoothness analysis of subdivision schemes by proximity," *Constr. Approx.* **24**, 289–318 (2006).
68. J. Wallner and N. Dyn, "Convergence and C^1 Analysis of Subdivision Schemes on Manifolds by Proximity," *Comput. Aided Geom. Des.* **22**, 593–622 (2005).
69. M. Zefran, V. Kumar and C. Croke, "Choice of Riemannian metrics for rigid body dynamics," *Proceedings of the ASME Design Engineering Technical Conference and Computers in Engineering Conf.,* Irvine, CA (Aug. 18–22, 1996) pp. 1–11.
70. M. Zefran and V. Kumar, "Planning of Smooth Motions on SE(3)," *Proceedings of the IEEE International Conf. on Robotics and Automation, Minneapolis, MN* (1996).
71. M. Zefran and V. Kumar, "Two Methods for Interpolating Rigid Body Motions," *Proceedings of the IEEE International Conf. on Robotics and Automation, Leuven, Belgium* (1996).
72. M. Zefran and V. Kumar, "Interpolation schemes for rigid body motions," *Comput. Aided Des.* **30**(3), 179–189 (1998).
73. M. Zefran, V. Kumar and C. Croke, "On the generation of smooth three-dimensional body motions," *IEEE Trans. Robot. Autom.* **14**, 576–589 (1998).

https://doi.org/10.1017/S0263574707003669 Published online by Cambridge University Press